A Simplified Zero-Forcing Receiver for Multi-User Uplink Systems Based on CB-OSFB Modulation

Xin Bian[1,2], Jinfeng Tian[2], Hong Wang[1], Mingqi Li[2], and Rongfang Song[1,3*]
[1] School of Communications and Information Engineering, Nanjing University of Posts and Telecommunications
Nanjing, Jiangsu, 210003, China
[e-mail: bianxin03@126.com]
[2] Shanghai Advanced Research Institute, Chinese Academy of Sciences
Shanghai, 201210, China
[e-mail: {tianjf, limq}@sari.ac.cn]
[3] Jiangsu Engineering Research Center of Communication and Network Technology, Nanjing University of Posts and Telecommunications
Nanjing, Jiangsu, 210003, China
[e-mail: songrf@njupt.edu.cn]
*Corresponding author: Rongfang Song

Received May 21, 2019; revised November 14, 2019; accepted March 18, 2020; published May 31, 2020

Abstract

This paper focuses on the simplified receiver design for multi-user circular block oversampled filter bank (CB-OSFB) uplink systems. Through application of discrete Fourier transform (DFT), the special banded structure and circular properties of the modulation matrix in the frequency domain of each user are derived. By exploiting the newly derived properties, a simplified zero-forcing (ZF) receiver is proposed for multi-user CB-OSFB uplink systems in the multipath channels. In the proposed receiver, the matrix inversion operation of the large dimension multi-user equivalent channel matrix is transformed into DFTs and smaller size matrix inversion operations. Simulation is given to show that the proposed ZF receiver can dramatically reduce the computational complexity while with almost the same symbol error rate as that of the traditional ZF receiver.

Keywords: Filter bank, oversampled filter bank, circular block, ZF receiver, uplink

This work was supported in part by the Science and Technology Commission of Shanghai Municipality under Grant 18DZ2203900, in part by the Shanghai Excellent Academic Leader Program under Grant 18XD1404100, in part by the National Key R&D Project of China under Grant 2019YFB1802703, in part by the Natural Science Foundation of Jiangsu Province under Grant BK20181392, in part by the Open Research Fund of Jiangsu Engineering Research Center of Communication and Network Technology, NJUPT, in part by the National Natural Science Foundation of China under Grant 61801246, and in part by Natural Science Foundation of Jiangsu Province under Grant BK20170910.

http://doi.org/10.3837/tiis.2020.05.023 **ISSN : 1976-7277**

1. Introduction

Due to its sensitivity to timing and frequency synchronization offset and high out-of-band (OOB) leakage, it is very essential to explore alternative solutions other than orthogonal frequency division multiplexing (OFDM) in order to meet the needs of future mobile communications such as massive machine-type communication (mMTC) and high spectral efficiency [1], [2], [3]. Recently, filter bank modulation (FBM) has received extensive attention from academic and industry for its low OOB emission and robustness to asynchronous transmission, which is proved to be a promising multi-carrier modulation scheme.

FBM techniques can be generally divided into two categories, i.e., critically sampled filter bank (CSFB) modulation technique and oversampled filter bank (OSFB) modulation technique. In a CSFB system, the perfect reconstruction only holds for a rectangular prototype filter while in an OSFB system, an over-sampling on each subcarrier is introduced so that the additional degree of freedom can be utilized for some better designed prototype filters. From the perspective of signal spectral property, sub-channel spacing of OSFB is larger than the sub-channel Nyquist band, thus reducing the inter-carrier interference (ICI).

There are already several OSFB schemes in the literature, e.g., filtered multitone (FMT) [4] which uses linear convolutions, cyclic block FMT (CB-FMT) [5], [6], [7], generalized multi-carrier (GMC) [8], and discrete frequency transformation spread GMC (DFT-S-GMC) [9] which exploit cyclic convolutions directly or equivalently with the data symbols transmitted in blocks, called circular block oversampled filter bank (CB-OSFB) in this paper. Because of the high computational complexity required for the direct implementation of OSFB, the low complexity receivers have been studied in the literature. In [7] and [10], the efficient time/frequency domain implementation structures of transceivers are explored, however, the receivers designed in the aforementioned works are only suitable for scenarios where a single user occupies the whole frequency components. Since the multi-path fading channels experienced by different users arriving at the receiver side are very different, meanwhile the number of occupied subcarriers of each user is not the same, the single-user low complexity receiving algorithms proposed in the literature cannot be directly promoted to the multi-user uplink access systems. Although the multi-user scenario performances have been evaluated in [9], it is only a special case where the channel matrices of multiple users are the same.

In this paper, a low-complexity multi-user ZF receiver based on CB-OSFB modulation is explored. The inversion of the original large-dimensional multi-user equivalent channel matrices is transformed into low-dimensional DFTs and smaller matrices by resorting to the subband sparsity property of the frequency-domain modulation matrix and the block cyclic characteristic of the matched-filtering Gram matrix, which significantly reduces the computational complexity. Simulation results show that, compared to the traditional ZF receiver, the symbol error rate (SER) performance loss of the system is very small when the number of subcarriers is large. It is worth mentioning that there are several linear receivers such as matched filter (MF), ZF, and minimum mean square error (MMSE) receivers that can be exploited [11]. The reason why the ZF receiver is effective is that ZF receiver can completely eliminate the ICI. Moreover, although with noise enhancement effect, the performance of ZF receiver approaches that of the MMSE receiver at high signal-to-noise ratios (SNRs).

The rest of this paper is organized as follows. The system model of CB-OSFB transmission is introduced in Section 2. The low-complexity ZF receiver is described in Section 3. Simulation results are given to validate the effectiveness of the proposed ZF receiver in Section 4. Conclusion is stated in Section 5.

Notations: Boldface uppercase, boldface lowercase, and normal letters are respectively denote matrices, vectors, and scalar quantities. $\mathbf{A}^H$ and $\mathbf{A}^{-1}$ signify the Hermitian transpose and inverse of matrix $\mathbf{A}$, respectively. $\mathbf{a}(m)$, $\mathbf{A}[m]$, and $[\mathbf{A}]_{m,n}$ stand for the m-th element of vector $\mathbf{a}$, m-th column of matrix $\mathbf{A}$, and (m,n)-th element of matrix $\mathbf{A}$, respectively. $|\aleph|$ expresses the cardinality of set $\aleph$. $\Delta^{M\times N}$ denotes the M rows and N columns set of complex matrices. $((\cdot))_L$ expresses the modulo-L operations, "$\otimes$" denotes the Kronecker operator, $\mathbf{I}_N$ and $\mathbf{0}_{M\times N}$ denote the identity matrix of size $N\times N$ and the zero matrix of size $M\times N$, respectively. $\mathbf{W}^{(N)}$ is the N-point DFT matrix with the (n,k)-th entry $\left[\mathbf{W}^{(N)}\right]_{n,k} = \exp\left(-j2\pi(n-1)(k-1)/K\right)/\sqrt{K}$.

2. System model for CB-OSFB modulation

Consider a K-user CB-OSFB uplink transmission system with the total number of N subcarriers that includes M symbols in each CB-OSFB block. The upsampling factor for CB-OSFB systems is N_s with N_s greater than N. $|\aleph_k|$ contiguous subcarriers with subcarrier index set $\aleph_k = \left\{k_1,...,k_{|\aleph_k|}\right\}$ are occupied for the k-th user. There exists a guard subcarrier between two adjacent sets. $\left\{g(l), l=0,...,L-1\right\}$ is the prototype filter used in CB-OSFB systems with $L = N_s M$.

The CB-OSFB modulation signal of user k can be expressed as

$$x_k(l) = \sum_{n\in\aleph_k}\sum_{m=0}^{M-1} s_{k,n}(m)\, p_{n,m}(l), l=0,...,L-1, \tag{1}$$

where $s_{k,n}(m)$ stands for the data symbols of user k transmitted on the n-th subcarrier in the m-th slot, $p_{n,m}(l)$ represents the circularly shifted version by mN_s of the n-th subcarrier filter coefficients given by

$$p_{n,m}(l) = g\left((l-mN_s)\right)_L \exp\left(j2\pi nl/N\right). \tag{2}$$

Then, the CB-OSFB modulation signal of user k can be rewritten as

$$\mathbf{x}_k = \mathbf{P}_k\mathbf{s}_k, \tag{3}$$

where $\mathbf{s}_k = \left[\mathbf{s}_{k,1}^T,...,\mathbf{s}_{k,|\aleph_k|}^T\right]^T$ denotes the transmitted symbol vector of user k with $\mathbf{s}_{k,n} = \left[s_{k,k_n}(0),...,s_{k,k_n}(M-1)\right]^T$, and $\mathbf{P}_k$ is the modulation matrix of user k, given by

$$\mathbf{P}_k = \left[\mathbf{\Phi}_{k_1}\mathbf{G}, \mathbf{\Phi}_{k_2}\mathbf{G}, ..., \mathbf{\Phi}_{k_{|\aleph_k|}}\mathbf{G}\right], \tag{4}$$

where $\mathbf{G}=\left[\mathbf{g},\mathbf{g}_{((N_s))},...,\mathbf{g}_{((M-1)N_s))}\right]\in\Delta^{L\times M}$ is the $L\times M$ subcarrier filtering matrix whose first column is the prototype filter vector $\mathbf{g}=\left[g(0),g(1),...,g(L-1)\right]^T$, $\mathbf{g}_{((mN_s))}$ corresponds to an mN_s -sample circularly shifted version of the prototype filter $\mathbf{g}$, and $\mathbf{\Phi}_i = diag\left\{1,\exp\left\{j2\pi i/N\right\},...,\exp\left\{j2\pi i(N_sM-1)/N\right\}\right\}$.

In CB-OSFB systems, a cyclic prefix (CP) which is longer than the channel spread delay is added to the beginning of the CB-OSFB block at the transmitter to cancel the wireless channel impairments. The CP-added transmit signal of user k then pass a multipath fading channel with a (L_c+1)-tap channel impulse response $\left[h_{k,0},...,h_{k,L_c}\right]^T$, where $\{h_{k,l}\}$ are i.i.d. Gaussian process with zero mean. In this paper, the channel impulse response (CIR) is assumed to remain unchanged in one CB-OSFB transmit block. At the receiver, the received signal after the removal of CP can be denoted as

$$\mathbf{y}=\sum_{k=1}^{K}\mathbf{H}_k\mathbf{P}_k\mathbf{s}_k+\mathbf{n}, \tag{5}$$

where $\mathbf{H}_k$ is the circulant CIR matrix of user k whose first column can be denoted as $\left[h_{k,0},...,h_{k,L_c},0,...,0\right]^T\in\Delta^{L\times 1}$. $\mathbf{n}$ stands for an additive white Gaussian noise vector with zero mean and variance σ_n^2.

We concentrate on the ZF receiver in this paper. Formula (5) can be rewritten compactly as

$$\mathbf{y}=\mathbf{H}_{eq}\mathbf{s}+\mathbf{n}, \tag{6}$$

where $\mathbf{H}_{eq}=\left[\mathbf{H}_1\mathbf{P}_1,...,\mathbf{H}_K\mathbf{P}_K\right]$ denotes the equivalent system matrix, and $\mathbf{s}=\left[\mathbf{s}_1^T,...,\mathbf{s}_K^T\right]^T$ denotes all the transmitted symbols of K users. With the assumption of perfect synchronization and channel estimate, at the receiver, the equalized signal can be obtained as

$$\hat{\mathbf{s}}=\mathbf{R}\mathbf{H}_{eq}\mathbf{s}+\mathbf{R}\mathbf{n}, \tag{7}$$

where $\mathbf{R}$ is the equalizer matrix. The traditional ZF equalizer for $\mathbf{R}$ is

$$\mathbf{R}_{ZF}=\left(\mathbf{H}_{eq}^H\mathbf{H}_{eq}\right)^{-1}\mathbf{H}_{eq}^H. \tag{8}$$

Direct matrix multiplications and inversions in (8) demand a very large computational complexity, especially when the dimension of matrices is large, which may not be affordable in practical situations. Therefore, low complexity ZF receiver techniques will be explored in the reminder of this paper that can substantially reduce the computational cost.

3. Proposed ZF receiver

In this section, we first derive the properties of the frequency-domain modulation matrix by taking advantage of the particular structure of the modulation matrix. Then, simplified ZF receiver design on the basis of the derived properties is developed. Finally, analysis of the computational cost of the proposed ZF and traditional ZF receivers is given.

3.1 Frequency domain structures of the modulation matrix

Transform the subcarrier filtering matrix $\mathbf{G}$ into the frequency domain, we can obtain

$$\hat{\mathbf{G}} = \mathbf{W}^{(N_S M)}\mathbf{G}, \tag{9}$$

whose first column is given by $\hat{\mathbf{g}} = \mathbf{W}^{(N_S M)}\mathbf{g}$, which is the frequency response of the prototype filter.

In practice, the root raised cosine (RRC) filter and the raised cosine (RC) with roll-off factor $\alpha < 1$ usually serve as the prototype filter, where there are at most $2Q$ nonzero frequency components with $L = N_s M = NQ$. Furthermore, since additional guard band is introduced between two adjacent subbands, ICI in CB-OSFB systems is much smaller than that in corresponding CSFB systems, thus it is reasonable to use only Q non-zero frequency components to approximate the prototype filter. In this paper, RC filter is adopted to act as the prototype filter. Therefore, low complexity ZF receiver design for the case of $2Q$ nonzero frequency components and the case of Q non-zero frequency components will be analyzed respectively.

3.1.1 Case 1: $2Q$ nonzero frequency components

The characteristics of the frequency-domain subcarrier filtering matrix $\hat{\mathbf{G}}$ together with the frequency-domain modulation matrix $\hat{\mathbf{P}}_k$ are given in the following two propositions, respectively.

Proposition 1: *The frequency-domain subcarrier filtering matrix* $\hat{\mathbf{G}}$ *can be divided into* N *subblocks as* $\hat{\mathbf{G}} = \left[\hat{\mathbf{G}}_1^T, \mathbf{0}_{Q\times M}, ..., \mathbf{0}_{Q\times M}, \hat{\mathbf{G}}_N^T\right]^T$ *with* $\hat{\mathbf{G}}_1$ *and* $\hat{\mathbf{G}}_N$ *denoted as*

$$\hat{\mathbf{G}}_1 = \sqrt{M}\boldsymbol{\Gamma}_1\boldsymbol{\Pi}_1\mathbf{W}^{(M)}, \tag{10}$$

$$\hat{\mathbf{G}}_N = \sqrt{M}\boldsymbol{\Gamma}_N\boldsymbol{\Pi}_N\mathbf{W}^{(M)}, \tag{11}$$

respectively, where $\boldsymbol{\Gamma}_1 = diag\left\{\hat{\mathbf{g}}(0), ..., \hat{\mathbf{g}}(Q-1)\right\}$, $\boldsymbol{\Gamma}_N = diag\left\{\hat{\mathbf{g}}(L-Q), ..., \hat{\mathbf{g}}(L-1)\right\}$, $\boldsymbol{\Pi}_1 = \left[\mathbf{I}_M; \mathbf{I}_{Q-M}\ \mathbf{0}_{(Q-M)\times(2M-Q)}\right] \in \Delta^{Q\times M}$, *and* $\boldsymbol{\Pi}_N = \left[\mathbf{0}_{(Q-M)\times(2M-Q)}\ \mathbf{I}_{Q-M}; \mathbf{I}_M\right] \in \Delta^{Q\times M}$.

Proof: As these $2Q$ nonzero frequency coefficients are distributed in the range of $[0, ..., Q-1]$ and $[L-Q, ..., L-1]$, we can derive

$$\hat{\mathbf{g}}(n) = 0, \quad Q < n < L-Q. \tag{12}$$

Using the property of DFT that the cyclic shift in time is the phase shift in the frequency domain, we can obtain

$$\hat{\mathbf{g}}_l = \mathbf{W}^{(L)}\mathbf{g}_{((lN_s))} = \hat{\mathbf{g}} * \theta_l, \tag{13}$$

where the phase shift vector $\theta_l = \left[\exp\left\{-j\frac{2\pi l 0}{M}\right\}, ..., \exp\left\{-j\frac{2\pi l(L-1)}{M}\right\}\right]^T$, and " $*$ " expresses the element-wise product operator.

Substituting (13) into (9), we can obtain

$$\hat{\mathbf{G}} = \left[\hat{\mathbf{g}}, \hat{\mathbf{g}}_1, ..., \hat{\mathbf{g}}_{M-1}\right] = diag\{\hat{\mathbf{g}}\}\boldsymbol{\Theta}, \tag{14}$$

where $\mathbf{\Theta} \in \Delta^{N_s M \times M}$ is the $N_s M \times M$ phase shift matrix whose (l,m) -th element is $[\mathbf{\Theta}]_{l,m} = \exp\left\{-j\frac{2\pi(l-1)(m-1)}{M}\right\}$. Substituting (12) into (14), we can obtain Proposition 1. The proof is completed.

On the basis of the definition that the frequency-domain modulation matrix of user k

$$\hat{\mathbf{P}}_k = \mathbf{W}^{(N_s M)}\mathbf{P}_k = \left[\mathbf{W}^{(N_s M)}\mathbf{\Phi}_{k_1}\mathbf{G},...,\mathbf{W}^{(N_s M)}\mathbf{\Phi}_{k_{|\aleph_k|}}\mathbf{G}\right], \tag{15}$$

we can derive the following proposition.

Proposition 2: *In the case of the subcarrier allocation method mentioned in Section 2, the frequency-domain modulation matrix* $\hat{\mathbf{P}}_k$ *can be denoted as*

$$\hat{\mathbf{P}}_k = \left[\mathbf{0}_{|\aleph_k|M\times(k_1-1)Q}, \mathbf{D}_k^T, \mathbf{0}_{|\aleph_k|M\times(N-|\aleph_k|-k_1)Q}\right]^T, \tag{16}$$

where the rectangular matrix $\mathbf{D}_k \in \Delta^{(|\aleph_k|+1)Q\times|\aleph_k|M}$ *is expressed as*

$$\mathbf{D}_k = \begin{bmatrix} \hat{\mathbf{G}}_N & \mathbf{0} & \cdots & \mathbf{0} \\ \hat{\mathbf{G}}_1 & \hat{\mathbf{G}}_N & \ddots & \vdots \\ \mathbf{0} & \ddots & \ddots & \mathbf{0} \\ \vdots & \ddots & \hat{\mathbf{G}}_1 & \hat{\mathbf{G}}_N \\ \mathbf{0} & \cdots & \mathbf{0} & \hat{\mathbf{G}}_1 \end{bmatrix}. \tag{17}$$

Proof: Note that, the i -th block in (15) can be denoted as

$$\mathbf{W}^{(N_s M)}\mathbf{\Phi}_{k_1}\mathbf{G} = \mathbf{W}^{(N_s M)}\mathbf{\Phi}_{k_1}\mathbf{W}^{(N_s M)H}\hat{\mathbf{G}}. \tag{18}$$

The (l,m) -th element of $\mathbf{W}^{(N_s M)}\mathbf{\Phi}_{k_i}\mathbf{W}^{(N_s M)H}$ can be given by

$$\begin{aligned} &\left[\mathbf{W}^{(N_s M)}\mathbf{\Phi}_{k_i}\mathbf{W}^{(N_s M)H}\right]_{l,m} \\ &= \left(\mathbf{W}^{(N_s M)}[l]\right)^T \mathbf{\Phi}_{k_i}\left(\mathbf{W}^{(N_s M)}[m]\right)^* \\ &= \frac{1}{N_s M}\sum_{n=0}^{N_s M-1}\exp\left\{-j2\pi n\frac{l-k_i N_s - m}{N_s M}\right\} \\ &= \begin{cases} 1, & m = (l-k_i N_s)_{N_s M}, l = 1,...,N_s M, \\ 0, & \textit{otherwise}, \end{cases} \end{aligned} \tag{19}$$

where $\mathbf{W}^{(N_s M)}[l]$ expresses the l -th column of $\mathbf{W}^{(N_s M)}$. Thus, $\mathbf{W}^{(N_s M)}\mathbf{\Phi}_{k_i}\mathbf{W}^{(N_s M)H}$ is a circular shift matrix to shift the elements of a column vector downwards by $k_i N_s$. Then, based on the expression of $\hat{\mathbf{G}}$ in Proposition 1, the expression of $\hat{\mathbf{P}}_k$ is obtained.

3.1.2 Case 2: Q nonzero frequency components

When Q nonzero frequency components of the prototype in the frequency domain are utilized,

we first shift the prototype filter downwards by half a subband, i.e., $\mathbf{g}_b = diag\left\{1, \exp\left(-j\frac{2\pi\times 0.5}{N}\right), ..., \exp\left(-j\frac{2\pi\times 0.5\times(L-1)}{N}\right)\right\}\mathbf{g}$. Similarly, the properties of the frequency-domain subcarrier filtering matrix $\hat{\mathbf{G}}$ and the frequency-domain modulation matrix $\hat{\mathbf{P}}_k$ are given in the following two propositions, respectively.

Proposition 3: *The frequency-domain subcarrier filtering matrix* $\hat{\mathbf{G}}$ *can be divided into* N *subblocks as* $\hat{\mathbf{G}} = \left[\mathbf{0}_{Q\times M}, ..., \mathbf{0}_{Q\times M}, \hat{\mathbf{G}}_b^T\right]^T$ *with* $\hat{\mathbf{G}}_b$ *denoted as*

$$\hat{\mathbf{G}}_b = \sqrt{M}\boldsymbol{\Gamma}_b\boldsymbol{\Pi}_N\mathbf{W}^{(M)}, \tag{20}$$

where $\boldsymbol{\Gamma}_b = diag\left\{\mathbf{g}_b(L-Q), ..., \mathbf{g}_b(L-1)\right\}$, *and* $\boldsymbol{\Pi}_N = \left[\mathbf{0}_{(Q-M)\times(2M-Q)}\ \mathbf{I}_{Q-M}\ ;\mathbf{I}_M\right] \in \Delta^{Q\times M}$.

Proposition 4: *In the case of the subcarrier allocation method mentioned in Section 2, the frequency-domain modulation matrix* $\hat{\mathbf{P}}_k$ *can be denoted as*

$$\hat{\mathbf{P}}_k = \left[\mathbf{0}_{|\aleph_k|M\times(k_1-1)Q}, \mathbf{D}_k^T, \mathbf{0}_{|\aleph_k|M\times(N-|\aleph_k|-k_1)Q}\right]^T, \tag{21}$$

where the rectangular matrix $\mathbf{D}_k \in \Delta^{(|\aleph_k|+1)Q\times|\aleph_k|M}$ *is expressed as*

$$\mathbf{D}_k = \begin{bmatrix} \hat{\mathbf{G}}_b & \mathbf{0} & \cdots & \mathbf{0} \\ \mathbf{0} & \hat{\mathbf{G}}_b & \ddots & \vdots \\ \vdots & \ddots & \ddots & \mathbf{0} \\ \mathbf{0} & \cdots & \mathbf{0} & \hat{\mathbf{G}}_b \end{bmatrix}. \tag{22}$$

The proofs of Proposition 3 and Proposition 4 are similar to the former two Propositions, which are omitted here due to the space limitations.

3.2 Simplified receiver design procedures

3.2.1 Frequency domain transformation

Due to the factor that $\mathbf{H}_k$ is a circulant square matrix, it can be transformed into a diagonal matrix with the aid of the DFT matrix $\mathbf{W}^{(N_sM)}$ as

$$\mathbf{W}^{(N_sM)}\mathbf{H}_k\mathbf{W}^{(N_sM)H} = \boldsymbol{\Lambda}_k, \tag{23}$$

where $\boldsymbol{\Lambda}_k$ is the diagonal matrix with $\left[\boldsymbol{\Lambda}_k\right]_{n,n} = \sum_{l=0}^{L-1} h_{k,l}\exp\left\{-j2\pi\frac{nl}{N_sM}\right\}$ on its n-th diagonal. Then, the frequency-domain received signal can be denoted as

$$\hat{\mathbf{y}} = \mathbf{W}^{(N_sM)}\mathbf{y} = \sum_{k=1}^{K}\boldsymbol{\Lambda}_k\hat{\mathbf{P}}_k\mathbf{s}_k + \hat{\mathbf{n}}, \tag{24}$$

where $\hat{\mathbf{n}} = \mathbf{W}^{(N_sM)}\mathbf{n}$. Differently from single user CB-OSFB systems, the frequency-domain channel responses $\boldsymbol{\Lambda}_k$'s cannot be compensated for simultaneously in multi-user CB-OSFB uplink transmission systems because $\boldsymbol{\Lambda}_k^{-1}\boldsymbol{\Lambda}_{k'} \neq \mathbf{I}_{N_sM}, k' \neq k$.

3.2.2 Channel equalization for each user

Thanks to the special structure of $\hat{\mathbf{P}}_k$, the received signal of user k can be picked up from $\hat{\mathbf{y}}$ as

$$\begin{aligned}\hat{\mathbf{y}}_k &= \left[\hat{\mathbf{y}}\left(k_1 Q-Q+1\right),...,\hat{\mathbf{y}}\left(k_{|\aleph_k|}+1\right)Q\right]^T \\ &= \hat{\mathbf{\Lambda}}_k \mathbf{D}_k \mathbf{s}_k + \hat{\mathbf{n}}_k,\end{aligned} \tag{25}$$

where $\hat{\mathbf{\Lambda}}_k$ is a submatrix of $\mathbf{\Lambda}_k$, denoted as

$$\hat{\mathbf{\Lambda}}_k = diag\left\{\left[\mathbf{\Lambda}_k\right]_{\left(k_1 Q-Q+1\right),\left(k_1 Q-Q+1\right)},...,\left[\mathbf{\Lambda}_k\right]_{\left(k_{|\aleph_k|}+1\right)Q,\left(k_{|\aleph_k|}+1\right)Q}\right\}. \tag{26}$$

After one-tap channel equalization, the equalized signal can be given as

$$\bar{\mathbf{y}}_k = \hat{\mathbf{\Lambda}}_k^{-1}\hat{\mathbf{y}}_k = \mathbf{D}_k \mathbf{s}_k + \bar{\mathbf{n}}_k, \tag{27}$$

where $\bar{\mathbf{n}}_k = \hat{\mathbf{\Lambda}}_k^{-1}\hat{\mathbf{n}}_k$.

3.2.3 Circulant matrix construction

Adding the last N_s elements of the vector $\bar{\mathbf{y}}_k$ to the first N_s elements of $\bar{\mathbf{y}}_k$, we then obtain a new vector with the length of $|\aleph_k| N_s$ as

$$\mathbf{z}_k = \bar{\mathbf{y}}_k^{(1)} + \bar{\mathbf{y}}_k^{(2)}, \tag{28}$$

where

$$\bar{\mathbf{y}}_k^{(1)} = \left[\bar{\mathbf{y}}_k(1),...,\bar{\mathbf{y}}_k\left(|\aleph_k| Q\right)\right]^T,$$

$$\bar{\mathbf{y}}_k^{(2)} = \left[\bar{\mathbf{y}}_k\left(|\aleph_k| Q+1\right),...,\bar{\mathbf{y}}_k\left(|\aleph_k| Q+Q\right),\mathbf{0}_{1\times\left(|\aleph_k| Q-Q\right)}\right]^T.$$

Substituting (27) to (28), we can derive

$$\mathbf{z}_k = \hat{\mathbf{D}}_k \mathbf{s}_k + \mathbf{v}_k, \tag{29}$$

where the i-th entry of noise vector $\mathbf{v}_k$ is

$$\mathbf{v}_k(i) = \begin{cases}\bar{\mathbf{n}}_k(i) + \bar{\mathbf{n}}_k\left(|\aleph_k| Q+i\right), & i=1,...,Q \\ \bar{\mathbf{n}}_k(i), & otherwise.\end{cases} \tag{30}$$

$\hat{\mathbf{D}}_k$ is a block-circulant matrix for user k with blocks of size $Q\times M$ whose first block column is denoted as $\left[\hat{\mathbf{G}}_N^T, \hat{\mathbf{G}}_1^T, \mathbf{0}_{M\times\left(|\aleph_k|-2\right)Q}\right]^T$ for Case 1 and $\left[\hat{\mathbf{G}}_b^T, \mathbf{0}_{M\times\left(|\aleph_k|-1\right)Q}\right]^T$ for Case 2.

3.2.4 Matched-filtering

Since $\hat{\mathbf{D}}_k \in \Delta^{Q|\aleph_k|\times M|\aleph_k|}$ is not a square matrix in CB-OSFB systems except the case that $Q=M$, we now consider the block-circulant square matrix $\mathbf{\Omega}_k = \hat{\mathbf{D}}_k^H \hat{\mathbf{D}}_k \in \Delta^{M|\aleph_k|\times M|\aleph_k|}$. For the case of $2Q$ non-zero frequency components, $\mathbf{\Omega}_k$ can be obtained as

$$\mathbf{\Omega}_k = \hat{\mathbf{D}}_k^H \hat{\mathbf{D}}_k = \begin{bmatrix} \hat{\mathbf{G}}_N^H \hat{\mathbf{G}}_N + \hat{\mathbf{G}}_1^H \hat{\mathbf{G}}_1 & \hat{\mathbf{G}}_1^H \hat{\mathbf{G}}_N & \cdots & \hat{\mathbf{G}}_N^H \hat{\mathbf{G}}_1 \\ \hat{\mathbf{G}}_N^H \hat{\mathbf{G}}_1 & \hat{\mathbf{G}}_N^H \hat{\mathbf{G}}_N + \hat{\mathbf{G}}_1^H \hat{\mathbf{G}}_1 & \ddots & \vdots \\ \vdots & \hat{\mathbf{G}}_N^H \hat{\mathbf{G}}_1 & \ddots & \hat{\mathbf{G}}_1^H \hat{\mathbf{G}}_N \\ \hat{\mathbf{G}}_1^H \hat{\mathbf{G}}_N & \cdots & \ddots & \hat{\mathbf{G}}_N^H \hat{\mathbf{G}}_N + \hat{\mathbf{G}}_1^H \hat{\mathbf{G}}_1 \end{bmatrix}. \tag{31}$$

For the case of Q non-zero frequency components, $\mathbf{\Omega}_k$ can be obtained as

$$\mathbf{\Omega}_k = \hat{\mathbf{D}}_k^H \hat{\mathbf{D}}_k = \begin{bmatrix} \hat{\mathbf{G}}_b^H \hat{\mathbf{G}}_b & \mathbf{0} & \cdots & \mathbf{0} \\ \mathbf{0} & \hat{\mathbf{G}}_b^H \hat{\mathbf{G}}_b & \ddots & \vdots \\ \vdots & \ddots & \ddots & \mathbf{0} \\ \mathbf{0} & \cdots & \mathbf{0} & \hat{\mathbf{G}}_b^H \hat{\mathbf{G}}_b \end{bmatrix}. \tag{32}$$

Therefore, the received signal after matched filtering operation can be rewritten as

$$\overline{\mathbf{z}}_k = \hat{\mathbf{D}}_k^H \mathbf{z}_k = \mathbf{\Omega}_k \mathbf{s}_k + \hat{\mathbf{D}}_k^H \mathbf{v}_k. \tag{33}$$

3.2.5 Equalization of the new block-circulant matrix

1) $2Q$ **nonzero frequency components**

Under the case of $2Q$ nonzero frequency components, the nonzero elements of $\mathbf{\Omega}_k$ can be expressed as

$$\hat{\mathbf{G}}_N^H \hat{\mathbf{G}}_1 = M\mathbf{W}^{(M)H} \left(\mathbf{\Pi}_N^H \mathbf{\Gamma}_N^H \mathbf{\Gamma}_1 \mathbf{\Pi}_1 \right) \mathbf{W}^{(M)}, \tag{34}$$

$$\hat{\mathbf{G}}_1^H \hat{\mathbf{G}}_N = M\mathbf{W}^{(M)H} \left(\mathbf{\Pi}_1^H \mathbf{\Gamma}_1^H \mathbf{\Gamma}_N \mathbf{\Pi}_N \right) \mathbf{W}^{(M)}, \tag{35}$$

and

$$\hat{\mathbf{G}}_N^H \hat{\mathbf{G}}_N + \hat{\mathbf{G}}_1^H \hat{\mathbf{G}}_1 = M\mathbf{W}^{(M)H} \left(\mathbf{\Pi}_N^H \mathbf{\Gamma}_N^H \mathbf{\Gamma}_N \mathbf{\Pi}_N + \mathbf{\Pi}_1^H \mathbf{\Gamma}_1^H \mathbf{\Gamma}_1 \mathbf{\Pi}_1 \right) \mathbf{W}^{(M)}, \tag{36}$$

respectively. Recall the block circular property of the matrix $\mathbf{\Omega}_k$, we can obtain

$$\mathbf{T}_k \mathbf{\Omega}_k \mathbf{T}_k^H = diag\left\{ \mathbf{B}_{k,0}, ..., \mathbf{B}_{k,|\aleph_k|-1} \right\}, \tag{37}$$

where

$$\mathbf{T}_k = \mathbf{W}^{(|\aleph_k|)} \otimes \mathbf{I}_M, \tag{38}$$

and $\mathbf{B}_{k,i}$ is denoted in (39). Substituting (34)-(36) into (39), we can derive $\mathbf{\Sigma}_{k,i}$ expressed in (40). $\mathbf{\Gamma}_1$, $\mathbf{\Gamma}_N$, $\mathbf{\Pi}_1$, and $\mathbf{\Pi}_N$ in (40) are given in the line below (11).

$$\begin{aligned} \mathbf{B}_{k,i} &= \hat{\mathbf{G}}_N^H \hat{\mathbf{G}}_N + \hat{\mathbf{G}}_1^H \hat{\mathbf{G}}_1 + \hat{\mathbf{G}}_N^H \hat{\mathbf{G}}_1 \exp\left\{ -j\frac{2\pi i}{|\aleph_k|} \right\} + \hat{\mathbf{G}}_1^H \hat{\mathbf{G}}_N \exp\left\{ -j\frac{2\pi \left(|\aleph_k| - 1 \right) i}{|\aleph_k|} \right\}. \\ &= \mathbf{W}^{(M)H} \mathbf{\Sigma}_{k,i} \mathbf{W}^{(M)} \end{aligned} \tag{39}$$

$$\begin{aligned} \mathbf{\Sigma}_{k,i} &= M\mathbf{\Pi}_N^H \mathbf{\Gamma}_N^H \mathbf{\Gamma}_N \mathbf{\Pi}_N + M\mathbf{\Pi}_1^H \mathbf{\Gamma}_1^H \mathbf{\Gamma}_1 \mathbf{\Pi}_1 \\ &+ M\exp\left\{ -j\frac{2\pi i}{|\aleph_k|} \right\} \mathbf{\Pi}_N^H \mathbf{\Gamma}_N^H \mathbf{\Gamma}_1 \mathbf{\Pi}_1 + M\exp\left\{ -j\frac{2\pi \left(|\aleph_k| - 1 \right) i}{|\aleph_k|} \right\} \left(\mathbf{\Pi}_1^H \mathbf{\Gamma}_1^H \mathbf{\Gamma}_N \mathbf{\Pi}_N \right). \end{aligned} \tag{40}$$

2) Q **nonzero frequency components**

Differently from the case of $2Q$ nonzero frequency components, in the case of Q nonzero frequency components, $\mathbf{\Sigma}_{k,i}$ is denoted as

$$\mathbf{\Sigma}_{k,i} = M\left(\mathbf{\Gamma}_N'^2 + \mathbf{\Gamma}_1'^2\right), \tag{41}$$

with $\mathbf{\Gamma}_1'^2$ and $\mathbf{\Gamma}_N'^2$ given in (42) and (43) respectively.

$$\left[\mathbf{\Gamma}_1'^2\right]_{i,i} = \begin{cases} \left[\mathbf{\Gamma}_1^2\right]_{ii} + \left[\mathbf{\Gamma}_1^2\right]_{i+M,i+M}, & 1 \le i \le Q-M, \\ \left[\mathbf{\Gamma}_1^2\right]_{ii}, & Q-M+1 \le i \le M. \end{cases} \tag{42}$$

$$\left[\mathbf{\Gamma}_N'^2\right]_{i,i} = \begin{cases} \left[\mathbf{\Gamma}_N^2\right]_{i+Q-M,i+Q-M}, & 1 \le i \le 2M-Q, \\ \left[\mathbf{\Gamma}_N^2\right]_{i+Q-M,i+Q-M} + \left[\mathbf{\Gamma}_N^2\right]_{i-(2M-Q),i-(2M-Q)}, & 2M-Q+1 \le i \le M. \end{cases} \tag{43}$$

Thus the recovered signal in (33) with ZF equalizer can be rewritten as

$$\hat{\mathbf{s}}_k = \mathbf{U}_k^H \mathbf{\Sigma}_k^{-1} \mathbf{U}_k \bar{\mathbf{z}}_k, \tag{44}$$

where $\mathbf{U}_k = diag\left\{\mathbf{W}^{(M)},...,\mathbf{W}^{(M)}\right\}\mathbf{T}_k$, $\mathbf{\Sigma}_k = diag\left\{\mathbf{\Sigma}_{k,0},...,\mathbf{\Sigma}_{k,|\aleph_k|-1}\right\}$, both $\mathbf{T}_k$ and $\mathbf{U}_k$ can be calculated by DFTs.

3.2.6 Summary of implementation

The summary of the implementation process of the proposed ZF equalizer can given as follows:

- **Step1:** Transform the CP-removed signal into the frequency domain by (24);
- **Step2:** Extract the received signal of each user by (25) and compensate for the channel impairments by (27);
- **Step3:** Build the block-circulant rectangular matrix by (28);
- **Step4:** Perform matched-filtering operation by (33);
- **Step5:** Conduct equalization on the block-circulant square matrix and recover the original signal by (44).

The flow chart of the proposed ZF receiver is shown in **Fig. 1**.

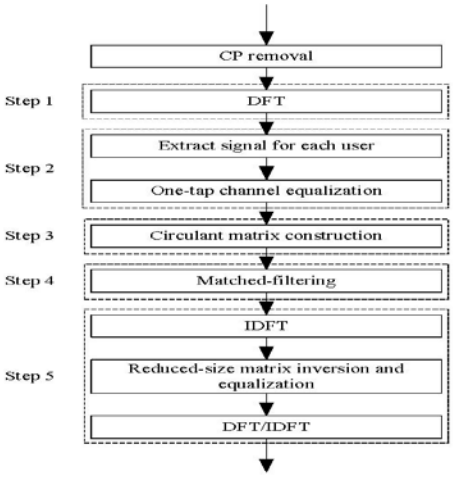

Fig. 1. Flow chart of the proposed ZF receiver.

3.3 Complexity analysis

Based on the number of complex multiplications (CMs), the computational complexity of our proposed ZF receiver structures is discussed, and compared to the traditional one. As described in the above subsection, our proposed ZF receiver involves five steps. The first step includes the N_sM -point DFT operations that requires $N_s^2M^2$ CMs. The second step is composed of the calculation of channel equalization which needs N_sM CMs and the calculation of diagonal elements in $\mathbf{\Lambda}_k$ which needs $N_sM\left(L_c+1\right)$ CMs. The multiplications with $\hat{\mathbf{D}}_k^H$ in the fourth step requires $\sum_{k=1}^{K}\left|\aleph_k\right|^2 N_sM$ CMs. In the fifth step, the multiplications with $\mathbf{U}_k$ can be implemented by M times $\left|\aleph_k\right|$-point DFT operations and $\left|\aleph_k\right|$ times M -point DFT operations which requires $\sum_{k=1}^{K}\left(M^2\left|\aleph_k\right|+M\left|\aleph_k\right|^2\right)$ CMs, $\mathbf{\Sigma}_k^{-1}$ can be realized by $\left|\aleph_k\right|$ times M -point matrix inverse operations which needs $\sum_{k=1}^{K}\left|\aleph_k\right|M^3$ CMs for Case 1 or $\left|\aleph_k\right|$ times M -point one-tap equalization operations which needs $\left|\aleph_k\right|M$ CMs for Case 2. Since the calculation of $\mathbf{\Sigma}_k^{-1}$ only depends on the prototype filter coefficients, they can be calculated offline. Thus, the total complex multiplications required for the proposed ZF receiver under Case 1 and Case 2 are

$$C_{PZF-2Q}=N_sM\left(N_sM+L_c+2\right)+\sum_{k=1}^{K}\left|\aleph_k\right|^2\left(N_sM+2M+M^2\right)+2JM^2+JM^3, \tag{45}$$

$$C_{PZF-Q}=N_sM\left(N_sM+L_c+2\right)+\sum_{k=1}^{K}\left|\aleph_k\right|^2\left(N_sM+2M\right)+2JM^2+JM, \tag{46}$$

respectively. Note that $J=\sum_{k=1}^{K}\left|\aleph_k\right|$.

The computational complexity required for the traditional ZF receiver is depicted as follows. The formation of $\mathbf{H}_{eq}$ requires $N_sM^2J\left(L_c+1\right)$ CMs. The multiplication of $\mathbf{H}_{eq}^H\mathbf{H}_{eq}$ involves $N_sM^3J^2/2$ CMs. The inverse of $\left(\mathbf{H}_{eq}^H\mathbf{H}_{eq}\right)^{-1}$ requires M^3J^3 CMs. The multiplication of $\left(\mathbf{H}_{eq}^H\mathbf{H}_{eq}\right)^{-1}\mathbf{H}_{eq}^H$ needs $N_sM^3J^2$ CMs. Finally, the recovery of the received signal requires N_sM^2J CMs. Thus, the total complex multiplications required for the traditional ZF receiver is

$$C_{TZF}=N_sM^2\left(L_c+2\right)J+3N_sM^3J^2/2+M^3J^3. \tag{47}$$

4. Simulation Results

Several simulation parameters are given below. The number of users is set $K=4$. An RC filter with roll-off factors of α =0.1, 0.5, and 0.9 is used to serve as the prototype filter. Each tap of the $\left(L_c+1\right)$-length channel impulse response $\left\{h_{k,l}\right\}$ is an i.i.d. Gaussian process with zero mean and variance η_l^2 weighted by an exponential power delay profile, i.e., $\sum_{l=0}^{L_c}\eta_l^2=\sum_{l=0}^{L_c}\eta_0^2\exp\left\{-l/4\right\}=1$, where η_0^2 is the normalized factor for the channel power gain. 16QAM modulation scheme is adopted. Equal Numbers of subcarriers assigned to users

is adopted. The traditional ZF receiver follows (8) while the proposed ZF receivers are according to (44). The difference between the 1-proposed ZF receiver and the 2-proposed one lies at different number of non-zero frequency components. For the 1-proposed ZF receiver, 2 Q -point non-zero frequency components is truncated and $\mathbf{D}_k$ follows (17); for the 2-proposed one, Q -point non-zero frequency components is retained and $\mathbf{D}_k$ is in accordance with (22).

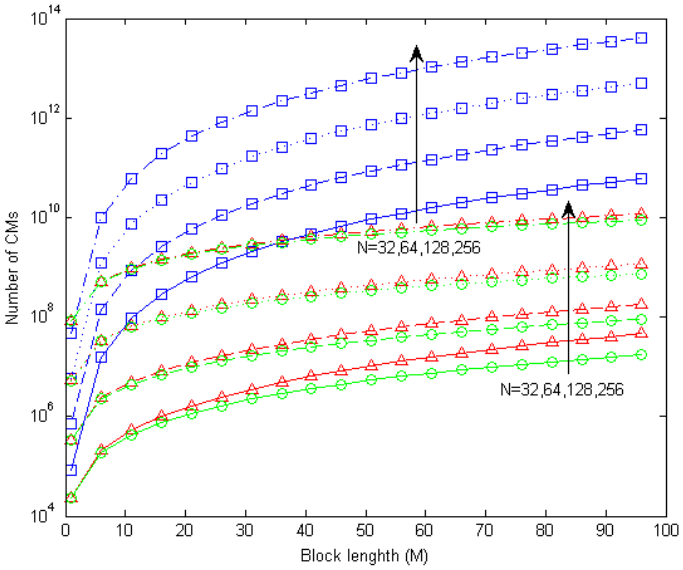

Fig. 2. Computational complexity comparison of different ZF receivers when $N \in [32, 64, 128, 256]$ and $M \in [1, 100]$. Equal Numbers of subcarriers assigned to users is adopted. 1-proposed ZF: proposed ZF receiver for Case 1, 2-proposed ZF: proposed ZF receiver for Case 2.

Fig. 2 shows the computational complexity comparison of the proposed ZF receiver with respect to the traditional ZF receiver when equal numbers of subcarriers are allocated to the users. The roll-off factor is 0.9. We can observe that, the computational multiplications required for the traditional ZF receiver are nearly 10^4 times that of the proposed ZF receiver, which indicates that the computational complexity required for the proposed schemes is significantly reduced. On the other hand, the computation cost required for the 2-proposed ZF is even less than that of the 1-proposed ZF. This is because the calculation of $\mathbf{\Sigma}_k^{-1}$ in the 2-proposed ZF doesn't involve the matrix inversion operation. Similar performance is achieved under unequal subcarrier allocations and omitted for simplicity.

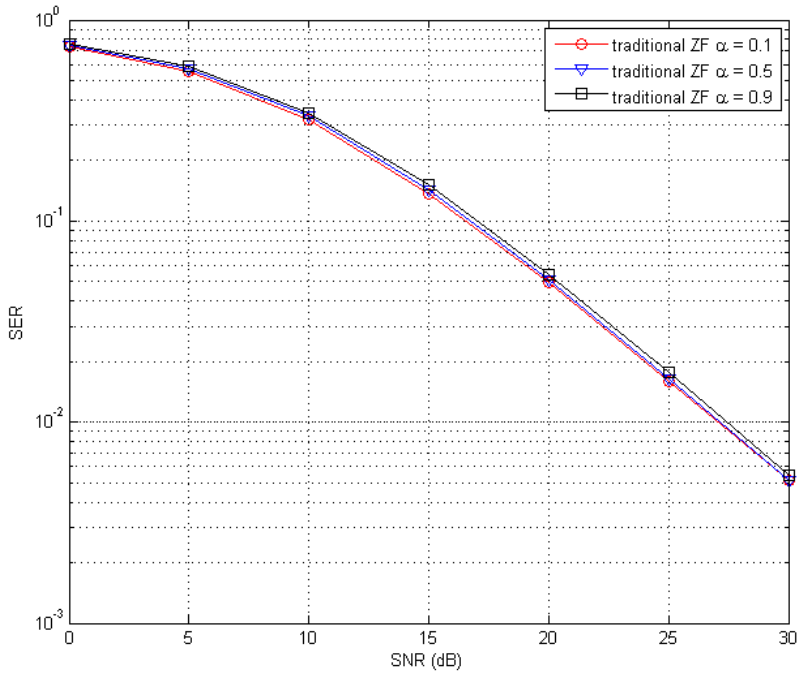

Fig. 3. SER performance for the traditional ZF receiver under different roll-off factors when $N = 256, N_s = 288, M = 8$. The subcarrier allocation schemes of the users are [63, 63, 63, 63].

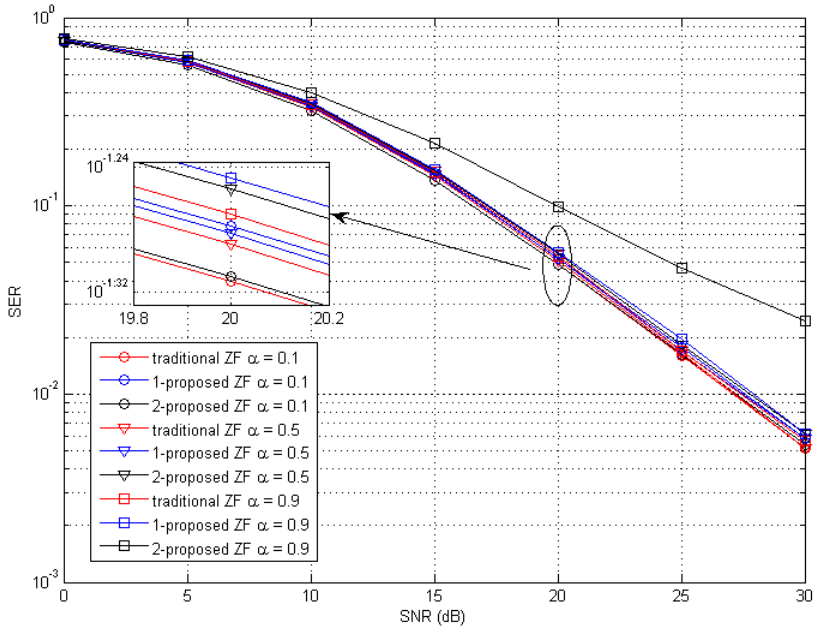

Fig. 4. SER performance for different ZF equalizers with $N = 256, N_s = 288, M = 8$. The subcarrier allocation schemes of the users are [63, 63, 63, 63].

Fig. 3 plots the system SER performance of the traditional ZF receiver under different roll-off factors with equal subcarrier assignment schemes. It can be observed that the SER performance under small roll-off factor outperforms that under the large one. This can be explained by the fact that the larger the roll-off factor is, the greater the overlap between subbands, which indicates the system will experience more ICI. On the other hand, if more guard band is introduced, i.e., by increasing the upsampling factor, the ICI that the system experiences will decrease, which can be verified in **Fig. 5**. We can observe from **Fig. 5** that the SER performances of three curves are almost the same.

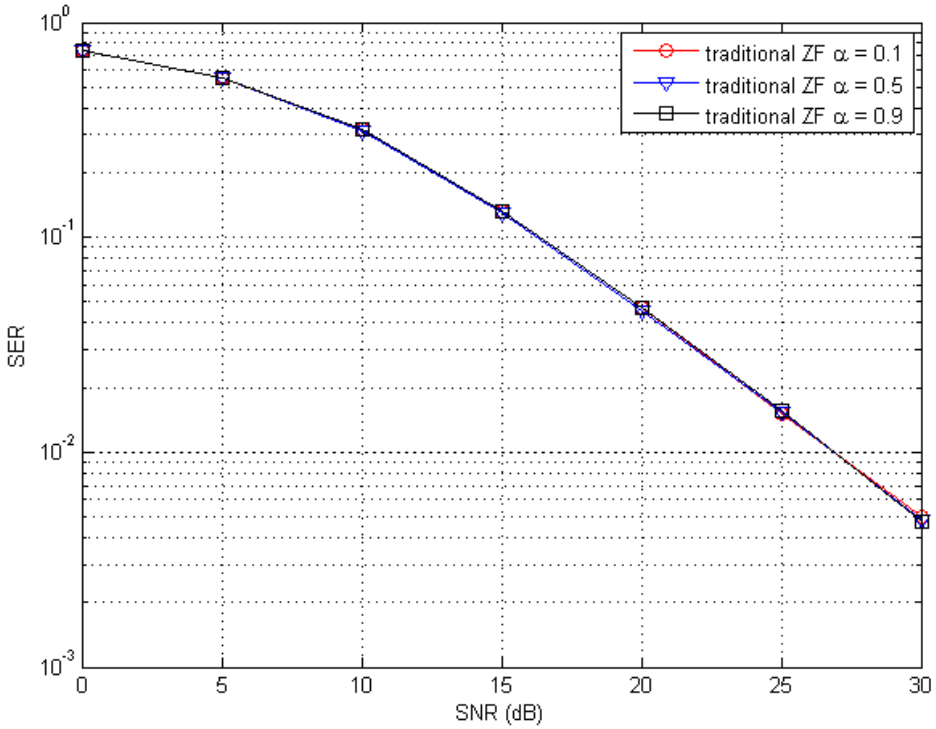

Fig. 5. SER performance under different roll-off factors when $N = 256, N_s = 320, M = 8$. The subcarrier allocation schemes of the users are [63, 63, 63, 63].

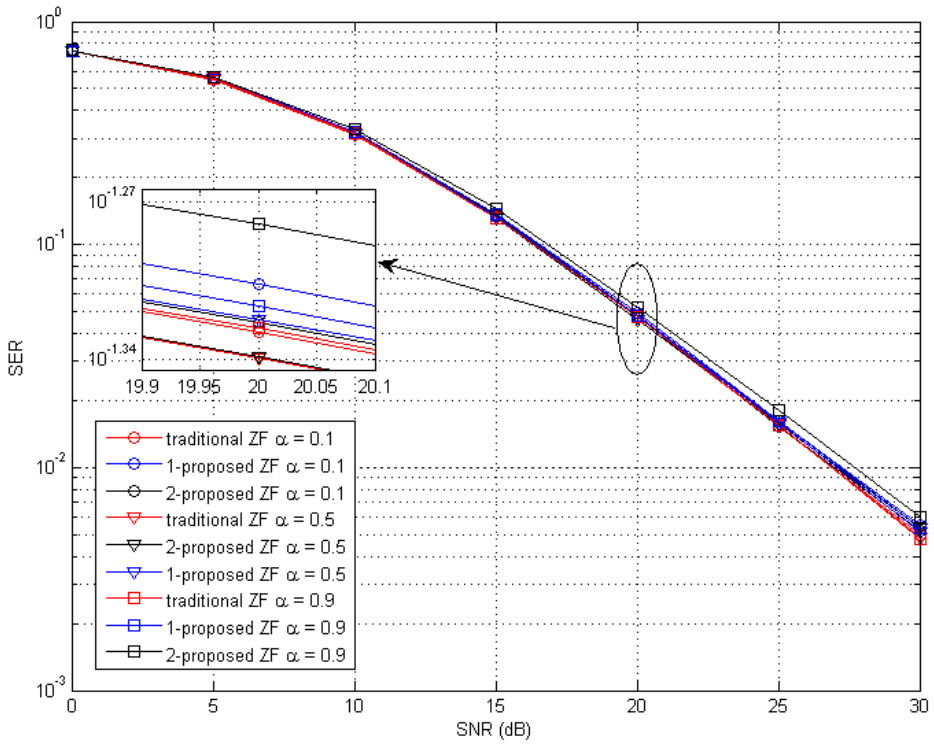

Fig. 6. SER performance for different ZF equalizers with $N = 256, N_s = 320, M = 8$. The subcarrier allocation schemes of the users are [63, 63, 63, 63].

The SER performances of the proposed and traditional ZF equalizers under different roll-off factors are illustrated in **Fig. 4**. We can observe from **Fig. 4** that the SER performance of the proposed ZF equalizer are approximately the same as that of the traditional ZF under equal subcarrier allocations. Note that there exists a small performance loss between the SER performance of the proposed ZF receiver and the traditional ZF receiver. The reason is that, the circulant matrix construction operation in the proposed ZF receiver brings about a larger noise power than that of the traditional ZF receiver after equalization, as is demonstrated in Appendix A. Moreover, in the case that the roll-off factor is 0.1, the 2-proposed ZF receiver performs slightly better than the 1-proposed one. This can be explained by the fact that Q-point nonzero frequency components adopted in the 2-proposed ZF receiver retain almost all the frequency domain energy of the prototype filter while having less noise power than the 1-proposed one. Furthermore, as the roll-off factor increases from 0.1 to 0.9, the system with 1-proposed ZF equalizer presents a better SER performance than that with 2-proposed ZF equalizer. This is because the larger the roll-off factor is, the flatter the subband spectrum is. In the case of large roll-off factor, taking the Q-point nonzero frequency components brings more truncation error than that in the case of small roll-off factor. Additionally, if we increase the over-sampling factor from 288 to 320, as shown in Fig.6, it is observed that for the roll-off factors of 0.1 and 0.5, the 2-proposed ZF receiver performs better than the 1-proposed one. This is due to that by increasing the sub-band guard interval, the ICI that the system experiences will decrease, thus the truncation error effect will decrease. Similar performances under unequal subcarrier allocations can be obtained and omitted for simplicity.

5. Conclusion

This paper proposes a simplified ZF receiver for multi-user CB-OSFB uplink systems. By taking advantage of the sparsity and block-circular structure of the frequency-domain modulation matrix, the computation of the large dimensional matrix inversion of equivalent channel matrix is transformed into DFT/IDFTs and smaller size matrix inversion operations. With the proposed ZF receiver, the computational cost of the system is dramatically simplified, meanwhile negligible SER performance loss is achieved. Simulation results are conducted to validate the analysis of our proposed low-complexity ZF receiver.

Appendix A. Proof of performance loss

It is observed that the simplification of the ZF receiver causes a minor performance loss. To demonstrate this, here we recall (27) and (29) as

$$\overline{\mathbf{y}}_k = \mathbf{D}_k \mathbf{s}_k + \overline{\mathbf{n}}_k, \tag{48}$$

and

$$\mathbf{z}_k = \hat{\mathbf{D}}_k \mathbf{s}_k + \mathbf{v}_k, \tag{49}$$

respectively. Note that, zero-forcing equalization can be applied to (48), which is equivalent to the traditional ZF receiver under the case that no more that $2Q$-point nonzero frequency components are utilized, while the zero-forcing equalization to (49) is the proposed ZF receiver. $\overline{\mathbf{n}}_k$ is an independent complex Gaussian random subvector of zero mean and variances $\{d_{k,i}\}$ with $d_{k,i} = \sigma_n^2 / \left[\hat{\mathbf{\Lambda}}_k\right]_{i,i}$ for $1 \le i \le |\aleph_k| Q + Q$. From (30), the variance of the i-th entry in $\mathbf{v}_k$ can be obtained as

$$q_{k,i} = \begin{cases} d_{k,i} + d_{k,|\aleph_k|Q+i}, & 1 \le i \le Q, \\ d_{k,i}, & Q < i \le |\aleph_k| Q + Q. \end{cases}$$

Additionally, $\mathbf{D}_k$ and $\hat{\mathbf{D}}_k$ are recalled as

$$\mathbf{D}_k = \begin{bmatrix} \hat{\mathbf{G}}_N & \mathbf{0} & \cdots & \mathbf{0} \\ \hat{\mathbf{G}}_1 & \hat{\mathbf{G}}_N & \ddots & \vdots \\ \mathbf{0} & \ddots & \ddots & \mathbf{0} \\ \vdots & \ddots & \hat{\mathbf{G}}_1 & \hat{\mathbf{G}}_N \\ \mathbf{0} & \cdots & \mathbf{0} & \hat{\mathbf{G}}_1 \end{bmatrix} \in \Delta^{(|\aleph_k|+1)Q \times |\aleph_k| M},$$

and

$$\hat{\mathbf{D}}_k = \begin{bmatrix} \hat{\mathbf{G}}_N & \mathbf{0} & \cdots & \hat{\mathbf{G}}_1 \\ \hat{\mathbf{G}}_1 & \hat{\mathbf{G}}_N & \ddots & \vdots \\ \vdots & \ddots & \ddots & \mathbf{0} \\ \mathbf{0} & \cdots & \hat{\mathbf{G}}_1 & \hat{\mathbf{G}}_N \end{bmatrix} \in \Delta^{(|\aleph_k|)Q \times |\aleph_k| M},$$

respectively.

To detect the data symbols of user k, let we denote $\mathbf{E}_k$ as the zero-forcing equalization matrix for equalizing $\hat{\mathbf{D}}_k$ of user k with $\mathbf{E}_k = \left[\mathbf{e}_{k,1},...,\mathbf{e}_{k,|\aleph_k|Q}\right]$. Then, we can obtain

$$\mathbf{e}_{k,i}^H \hat{\mathbf{D}}_k[j] = \begin{cases} 1, & j = i, \\ 0, & j \neq i. \end{cases} \tag{50}$$

where $\mathbf{e}_{k,i}$ is the i-th equalizing vector for equalizing $\hat{\mathbf{D}}_k$ of user k, $\hat{\mathbf{D}}_k[j]$ represents the j-th column of the matrix $\hat{\mathbf{D}}_k$. Then, after the circular matrix construction in (28), the i-th element of the noise power vector of user k can be derived as

$$\begin{aligned} \omega_{k,i}^{1-PZF} &= \sum_{n=1}^{|\aleph_k|Q} \left|\mathbf{e}_{k,i}(n)\right|^2 q_{k,n} \\ &= \sum_{n=1}^{|\aleph_k|Q} \left|\mathbf{e}_{k,i}(n)\right|^2 d_{k,n} + \sum_{n=1}^{Q} \left|\mathbf{e}_{k,i}(n)\right|^2 d_{k,|\aleph_k|Q+n}. \end{aligned}$$

Lemma A.1: *For the i-th data stream of user k, $\hat{\mathbf{e}}_{k,i} = \left[\mathbf{e}_{k,i}^T, \mathbf{a}_{k,i}^T\right]^T$ with $\mathbf{a}_{k,i} = \left[\mathbf{e}_{k,i}(1),..., \mathbf{e}_{k,i}(Q)\right]^T$ is one possible zero interference vector for (48), i.e.,*

$$\hat{\mathbf{e}}_{k,i}^H \mathbf{D}_k[j] = \begin{cases} 1, & j = i, \\ 0, & j \neq i. \end{cases} \tag{51}$$

Proof. For $1 \le i \le |\aleph_k|Q - Q$, by using (51), we have

$$\hat{\mathbf{e}}_{k,i}^H \mathbf{D}_k[j] = \mathbf{e}_{k,i}^H \hat{\mathbf{D}}_k[j] = \begin{cases} 1, & j = i, \\ 0, & j \neq i. \end{cases} \tag{52}$$

For $|\aleph_k|Q - Q + 1 \le i \le |\aleph_k|Q$, with (51), we can derive

$$\begin{aligned} &\left[\mathbf{e}_{k,i}(|\aleph_k|Q - Q + 1),..., \mathbf{e}_{k,i}(|\aleph_k|Q)\right]^H \hat{\mathbf{G}}_N[c] \\ &+\left[\mathbf{e}_{k,i}(1),..., \mathbf{e}_{k,i}(Q)\right]^H \hat{\mathbf{G}}_1[c] = \begin{cases} 1, & j = i, \\ 0, & j \neq i. \end{cases} \end{aligned} \tag{53}$$

where $c = j - (|\aleph_k| - 1|Q)$, $\hat{\mathbf{G}}_1[l]$ and $\hat{\mathbf{G}}_N[l]$ are the l-th columns of $\hat{\mathbf{G}}_1$ and $\hat{\mathbf{G}}_N$, respectively. Thus, Lemma 6.1 is proved.

By applying the zero interference vector $\hat{\mathbf{e}}_{k,i}$ to (48), the i-th entry of the noise power vector of user k can be derived as

$$\begin{aligned} \omega_{k,i}^{zero} &= \sum_{n=1}^{|\aleph_k|Q+Q} \left|\hat{\mathbf{e}}_{k,i}(n)\right|^2 d_{k,n} \\ &= \sum_{n=1}^{|\aleph_k|Q} \left|\mathbf{e}_{k,i}(n)\right|^2 d_{k,n} + \sum_{n=1}^{Q} \left|\mathbf{e}_{k,i}(n)\right|^2 d_{k,|\aleph_k|Q+n} \end{aligned} \tag{54}$$

Denote $\omega_{k,i}^{TZF}$ as the i-th element of the noise power vector of user k of the traditional ZF

receiver, then it can be inferred from the Guass-Markov theorem that the traditional ZF equalizing vector with least square solution has the minimum noise power among all the zero interference vectors [12], i.e.,

$$\omega_{k,i}^{TZF} \le \omega_{k,i}^{zero} = \omega_{k,i}^{1-PZF}. \tag{55}$$

Thus, we have demonstrated that the proposed simplified ZF receiver with circular matrix construction has a larger noise power than the traditional ZF receiver. Since the desired signal power is normalized after equalization, the signal-to-interference-plus-noise ratio (SINR) of the proposed ZF receiver is no more than the traditional ZF, which causes a performance loss of the proposed ZF receivers.

References

[1] A. Aminjavaheri, A. Farhang, A. RezazadehReyhani, and B. Farhang-Boroujeny, "Impact of timing and frequency offsets on multicarrier waveform candidates for 5G," in *Proc. of 2015 IEEE Signal Processing and Signal Processing Education Workshop (SP/SPE)*, pp. 178-183, August, 2015. Article (CrossRef Link)

[2] J. Van De Beek and F. Berggren, "Out-of-Band Power Suppression in OFDM," *IEEE Communications Letters*, vol. 12, no. 9, pp. 609-611, September, 2008. Article (CrossRef Link)

[3] X. Zhang, L. Chen, J. Qiu, and J. Abdoli, "On the Waveform for 5G," *IEEE Communications Magazine*, vol. 54, no. 11, pp. 74-80, November, 2016. Article (CrossRef Link)

[4] G. Cherubini, E. Eleftheriou, and S. Olcer, "Filtered multitone modulation for very high-speed digital subscriber lines," *IEEE Journal on Selected Areas in Communications*, vol. 20, no. 5, pp. 1016-1028, June, 2002. Article (CrossRef Link)

[5] A. M. Tonello, "A novel multi-carrier scheme: Cyclic block filtered multitone modulation," in *Proc. of 2013 IEEE International Conference on Communications (ICC)*, pp. 5263-5267, 2013. Article (CrossRef Link)

[6] A. M. Tonello, and M. Girotto, "Cyclic block FMT modulation for broadband power line communications," in *Proc. of 2013 IEEE 17th International Symposium on Power Line Communications and Its Applications*, pp. 247-251, 2013. Article (CrossRef Link)

[7] A. M. Tonello, and M. Girotto, "Cyclic block filtered multitone modulation," *EURASIP Journal on Advances in Signal Processing*, vol. 2014, no. 109, pp. 1-18, 2014. Article (CrossRef Link)

[8] X. Gao, X. You, B. Jiang, Z. Pan, and X. Wang, "Generalized multi-carrier transmission technique for beyond 3G mobile communications," in *Proc. of 2005 IEEE 16th International Symposium on Personal, Indoor and Mobile Radio Communications*, vol. 2, pp. 972-976, 2005. Article (CrossRef Link)

[9] X. Zhang, M. Li, H. Hu, H. Wang, B. Zhou, and X. You, "DFT Spread Generalized Multi-Carrier Scheme for Broadband Mobile Communications," in *Proc. of 2006 IEEE 17th International Symposium on Personal, Indoor and Mobile Radio Communications*, pp. 1-5, 2006. Article (CrossRef Link)

[10] Y. Rui, H. Hu, H. Yi, H. Chen, and Y. Huang, "Frequency domain discrete fourier transform spread generalized multi-carrier system and its performance analysis," *Computer Communications*, vol. 32, no.3, pp. 456 - 464, 2009. Article (CrossRef Link)

[11] A. Farhang, N. Marchetti, and L. E. Doyle, "Low-complexity modem design for GFDM," *IEEE Transactions on Signal Processing*, vol. 64, no. 6, pp. 1507–1518, March 2016. Article (CrossRef Link)

[12] X. Zhang, *Matrix Analysis and Applications*, Cambridge University Press, 2017. Article (CrossRef Link)

Xin Bian received the B.S. degree in telecommunications engineering from Anhui Normal University in 2011 and he is currently pursuing the Ph.D. degree in communication and information systems at Nanjing University of Posts and Telecommunications (NUPT). His research interests are in the areas of filter bank modulation and multiple access techniques.

Jinfeng Tian received the M.S. degree from University of Electronic Science and Technology of China (UESTC) in 2005, and the Ph.D. degree from Shanghai Institute of Microsystem and Information Technology (SIMIT), Chinese Academy of Sciences (CAS) in 2011, both in communications and information systems. From 2005 to 2008, she was with ZTE corporation in Shanghai and mainly engaged in the research of radio resource management. She joined Shanghai Advanced Research Institute (SARI), CAS in 2011 as an Associate Professor of Engineering. Her research interests include next generation broadcasting-wireless, 5G wireless communications, heterogeneous networks, parameter estimation, spectrum sensing, and statistical signal processing.

Hong Wang received the B.S. degree in Telecommunications Engineering from Jiangsu University, Zhenjiang, China, in 2011, and Ph.D. degree in the Department of Telecommunications Engineering from Nanjing University of Posts and Telecommunications (NUPT), Nanjing, China, in 2016. From 2014 to 2015, he was a Research Assistant with the Department of Electronic Engineering, City University of Hong Kong, Kowloon, Hong Kong. From 2016 to 2018, he was a Senior Research Associate with the State Key Laboratory of Millimeter Waves and Department of Electronic Engineering, City University of Hong Kong. Since Sep. 2016, he has also been an Instructor in Department of Telecommunication Engineering, NUPT. His research interests are in the area of broadband wireless communications, particularly in interference analysis and management in HetNets.

Mingqi Li received the Ph.D. degree in communication and information systems from Shanghai Jiaotong University in 2004 and he is currently a Professor and the Deputy Director of Research Center of Wireless Technologies for New Media, Shanghai Advanced Research Institute, Chinese Academy of Sciences. His research interests include filter bank modulation techniques, next generation broadcasting-wireless, 5G wireless communications.

Rongfang Song received the B.S. and M.S. degrees from the Nanjing University of Posts and Telecommunications (NUPT), Nanjing, China, in 1984 and 1989, respectively, and the Ph.D. degree from Southeast University, Nanjing, in 2001, all in electronic engineering. From 2002 to 2003, he was a Research Associate with the Department of Electronic Engineering, City University of Hong Kong, Hong Kong. Since 2002, he has been a Professor with the Department of Telecommunications Engineering, NUPT. His research interests are in the area of broadband wireless communications, with current focus on interference management in HetNets, non-orthogonal multiple access, and compressed sensing-based signal processing.